Solvent Quality, Phase Coexistence, and Dynamics in Ultrahigh Molecular Weight Diblock Copolymer Solutions

P. Holmqvist,[†] G. Fytas,*[,†] S. Pispas,[‡] N. Hadjichristidis,[‡] K. Saijo,[§] H. Tanaka,[§] and T. Hashimoto[§]

FORTH−Institute of Electronic Structure and Laser, P.O. Box 1527, 71110 Heraklion, Crete, Greece; Department of Chemistry, University of Athens, 15771 Zografou, Athens, Greece; and Department of Polymer Chemistry, Graduate School of Engineering, Kyoto University, Katsura, Kyoto 615-8510, Japan

Received February 12, 2004; Revised Manuscript Received April 14, 2004

ABSTRACT: The static $S(q)$ and dynamic $S(q,t)$ structure factor in disordered and ordered solutions of ultrahigh molecular mass (3.6×10^6 g/mol) symmetric poly(styrene)-*block*-poly(isoprene) (SI) diblock copolymer were measured by photon correlation spectroscopy for wave vectors q on both side of the maximum $S(q^*)$ as a function of concentration and temperature in two solvents. At ambient temperature, the SI concentration c_{ODT} at the disordered-to-ordered transition decreases with increasing solvent selectivity from toluene (4.2 wt %) to decaline (2.7 wt %). In the disordered region, deviation from solvent impartiality enhances and slows down the short ($q > q^*$) length order parameter fluctuations and hence leads to deviation of $S(q > q^*)$ from its theoretical mean-field form. From ultrasmall X-ray and light scattering, the $S(q)$ over a broad q range shows hexagonally arranged cylinders for the ordered solutions with decaline, suggesting a biased solvent partition in the two microphases. At c_{ODT}, a two-phase regime which is visually observed in both solvents due to light diffraction is comprised of two separated regions with different $S(q)$ and $S(q,t)$ only at the vicinity of q^*. For a rigorous interpretation of these effects, the solvent selectivity along with the renormalization of the neat block copolymer composition should be considered in the framework of the blob theory.

I. Introduction

Solvent selectivity is an important factor for the morphological phase behavior of amphiphilic molecules. There have been several reports on both the morphology and phase behavior covering numerous different block copolymers in solvent with ranging selectivity.[1−3] Few reports can be found, however, on the corresponding dynamic response[4] and no comparison, to our knowledge, of the dynamic response between systems with solvents of different selectivity. The practical use of selective solvent in amphiphilic systems, especially water, are far more important due to its environmental and biological properties than the model system of neutral, usually organic solvent used to characterize the system in our previous work. On the other hand, we have established a clear base for the understanding of the structure dynamics of diblock copolymers in neutral solvents.

To extend this understanding for a nonneutral solvency, a comparison of the dynamic behavior between a neutral and a slightly more selective solvent is addressed in this paper. The evolution of the dynamic behavior crossing the phase boundary from disordered-to-ordered regime (ODT) is still an untouched open question. Further, the presence of a two-phase region, well established in molecular amphiphilics,[5,6] is also conceivable in their macromolecular analogues when the solvent neutrality is slightly violated. A two-phase regime may be comprised of either a copolymer-rich and solvent-rich regions[7,8] or disordered and ordered regions;[9] these two alternatives may be interrelated. Albeit the disparity in the diblock copolymer concentration in the two-phase region at the transition is very small, substantial structural differences of the two phases should be manifested in their static $S(q)$ and probably dynamic $S(q,t)$ structure factor as a function of the wavevector q of the concentration fluctuations.

To properly address these questions, we use an ultrahigh molecular weight polystyrene-*block*-polyisoprene (SI) symmetric diblock copolymer in common neutral (toluene) and in slightly selective (decaline) solvent. The selectivity of the latter can be controlled by temperature. Both $S(q)$ and the structural relaxation function $S(q,t)$ on both side of $q^* = 2\pi/d$ (d is the characteristic Bragg spacing of the structure) were measured by photon correlation spectroscopy (PCS). The coexistence of an ordered and disordered phase is apparent by optical inspection as the grains in the former phase appear colored through the satisfaction of the light diffraction ($d \approx 325$ nm) condition. It turns out that apart from q in the vicinity of q^* both $S(q)$ and $S(q,t)$ of the two phases look alike.

II. Experimental Section

A. Polymer Synthesis. The ultrahigh molecular weight SI diblock was synthesized by high-vacuum anionic polymerization techniques[10] as described elsewhere.[4,11−14] Styrene was polymerized first, in benzene, using *sec*-BuLi as the initiator, followed by addition of isoprene. Since the concentration of the living PSLi is very low [M_n = (g of monomer)/(mol of *sec*-BuLi)], the unavoidable deactivation of PSLi by the tiny amount of impurities, accompanying isoprene, leads to an appreciable amount of PS homopolymer in the final reaction product. For this reason, three to five solvent/nonsolvent (toluene/methanol) fractionations were carried out,[12] depending on the molecular weight and composition of the block copolymer, for the removal of PS homopolymer and the isolation of pure diblocks; the present sample was five times fractionated. The weight-average molecular weight, M_w, of the fractionated diblock

[†] FORTH−Institute of Electronic Structure and Laser.
[‡] University of Athens.
[§] Kyoto University.

10.1021/ma049702p CCC: $27.50
Published on Web 06/04/2004

Table 1. Characteristic Properties of the Diblock Copolymer Solutions

solution	T/°C	$M_w \times 10^{-6}$ [a]	M_w/M_n	f_{PS}	c_{ODT}/ wt %	c_x/ wt %	q^*_{ODT}/nm^{-1} [b]
SI4M50/toluene	20	3.6	1.1	0.49	4.2	4.0	0.0194
SI4M50/decaline	20				2.9	1.7	0.0194
SI4M50/decaline	15				2.7	1.6	0.0194

[a] Reference 13. [b] At $c \sim c_{ODT}$.

copolymer SI4M50 was determined by low-angle laser light scattering, LALLS, in THF at 25 °C and the polydispersity index (M_w/M_n) by size exclusion chromatography, SEC, in THF at 40 °C. The average composition of the copolymers was determined by ^{1}H NMR spectroscopy in $CDCl_3$ at 30 °C. Characteristic quantities of this SI4M50 diblock solution in toluene and decaline are listed in Table 1. At the wavevector q^*, the light scattering intensity $I(q^*)$ assumes its maximum value and at the concentration c_{ODT} the SI4M50 solutions in toluene undergo the disorder-to-order transition (ODT) at 20 °C. The concentration c_{ODT} was estimated by the sudden change in $I(q^*)$, the width of the $I(q)$ distribution as a function of concentration[12,14] and visual inspection. At c_{ODT} the solution diffracts the white light and becomes colored at certain directions.

B. Photon Correlation Spectroscopy (PCS). The intermediate scattering function $C(q,t) = [(G(q,t) - 1)/f^*]^{1/2}$ is obtained from the experimental intensity autocorrelation function $G(q,t) = \langle I(q,t)I(q,0)\rangle/\langle I(q)\rangle^2$ (f^* is the instrumental coherence factor) measured by PCS in the polarized geometry under homodyne conditions over a broad time range (10^{-7}–10^2 s). The scattering wave vector $q = (4\pi n/\lambda)\sin(\theta/2)$ (λ is the laser wavelength in a vacuum, n is the solvent refractive index, and θ is the scattering angle in solution) ranges from 3×10^{-3} to 3.5×10^{-2} nm^{-1} in both toluene and decaline. An ALV-5000 full digital correlator was employed in conjunction with a Nd:YAG laser at $\lambda = 532$ nm. The measurements were carried out at 15 and 20 °C. The analysis of the high-quality intermediate scattering function $C(q,t)$ ($\propto S(q,t)$) proceeds via inverse Laplace transformation (ILT):

$$C(q,t) = \int L(\ln\tau;q)\exp(-t/\tau)\,\mathrm{d}(\ln\tau) \qquad (1)$$

In the present case, no assumption is made for the shape of the distribution of relaxation times at q, $L(\ln\tau;q)$, except that $C(q,t)$ is a sum of exponentials. The non-single-exponential shape of $C(q,t)$ is clearly revealed by the ILT leading to a nonunimodal distribution of the relaxation function $L(\ln\tau)$. The position and the area of each peak in $L(\ln\tau)$ define the rate, Γ_k, and intensity, $I_k = \alpha_k(q)I(q)$, of the kth process ($k = 1, 2, \ldots$), where

$$\alpha_k(q) = \frac{\int L_k(\ln\tau;\, q)\,\mathrm{d}\ln\tau}{\int L(\ln\tau;\, q)\,\mathrm{d}\ln\tau} \qquad (2)$$

is the fraction of $L(\ln\tau)$ associated with the kth process and $I(q)$ is the total intensity normalized to the polarized intensity of the solvent toluene.

C. USAXS. Ultrasmall X-ray scattering profile measurements were taken by using an apparatus detailed elsewhere[15] ($\lambda = 0.154$ nm) and with two step intervals with respect to q: 3.96×10^{-4} nm^{-1} and exposure time per step of 600 s (USAXS1) and 3.96×10^{-3} nm^{-1} and exposure time per step of 7000 s (USAXS2). The USAXS profiles were corrected for the slit-smearing effects and thermal diffusive scattering due to acoustic phonon contribution. At the largest q ($\sim$0.4 nm^{-1}) the latter contribution amounts to a small fraction of the total intensity, and hence the error subjected to this correction is very small.

III. Results and Discussion

A. Static Structure Factor. The static structure factor, $S(q) \propto I(q)/c$, for SI4M50 in decaline and toluene at concentrations equidistant to ODT, $c/c_{ODT} \simeq 0.36$, are presented in Figure 1. For the SI4M50/toluene solutions, the $S(q)$ are multiplied by a constant factor of 3.5 at all concentrations and temperatures (15 and 20 °C) in order to match the $S(q)$ of SI4M50/decaline solutions.[16] Surprisingly, the superposition of these renormalized structure factors for the disordered solutions fail in the region $q \geq q^*$. As the solvent selectivity increases from toluene to decaline at 20 °C and even more in decaline at 15 °C, the intensity increases only at $q > q^*$. The similarity in $S(q)$ at low q values and the disparity at $q > q^*$ suggest similar real-space morphology at large distances in the two solvents but a different local structure. It should be noted that decaline is not selective enough to create micelles, as for example decane and dimethylacetamide,[17] and hence $S(q)$ peaks at the same q^*. The formation of macroscopically homogeneous SI4M50 solutions in decaline is further indicated by the successful superposition of the $S(q)$ at large length scales ($q < q^*$) in Figure 1.

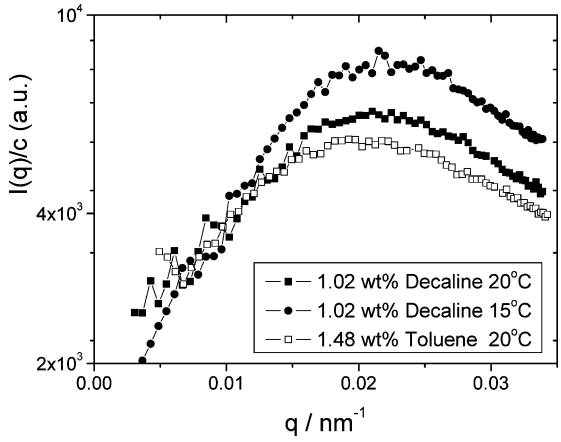

Figure 1. Intensity distribution $I(q)/c$ for disordered SI4M50 solutions in two different solvents: 1.48 wt % in toluene (○) at 20 °C and 1.02 wt % in decaline at 15 °C (■) and 20 °C (●). For the SI/toluene solution, the $I(q)/c$ is multiplied by 3.5 to match the $I(q)/c$ of the SI/decaline solution.

Since decaline is slightly selective, the solvent is no longer equally distributed between the two blocks, leading to extra fluctuations at smaller length scales (high q's). Hence, the solutions in decaline exhibit higher intensity, at $q > q^*$, than the corresponding solutions in toluene. The observed intensity changes, at $q > q^*$, for the solutions in decaline at 20 to 15 °C result from the strong variation of the solvent quality for the polystyrene block; the θ temperature of polystyrene in decaline is about 18 °C. The temperature matters much more for the phase state of the decaline solutions compared to the SI solutions in toluene where $S(q)$ is found to be insensitive to the temperature variations around the ambient temperature. Therefore, it is this temperature-dependent solvent quality that leads to the increase of $S(q^*)$ for the solutions in decaline with decreasing temperature in Figure 1. In this context, the unexpected lower c_{ODT} of the former decaline solution (Table 1) as compared to the same SI in toluene is also attributed to the solvent selectivity. In neutral solvents,

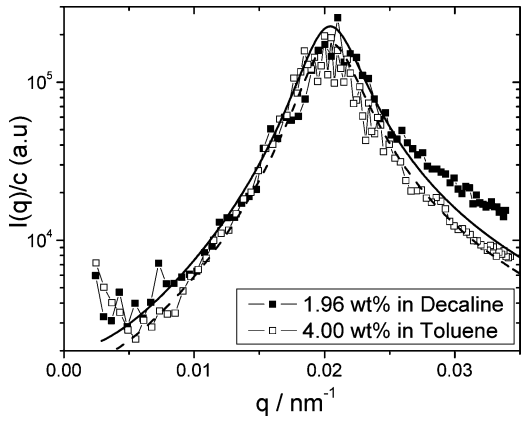

Figure 2. Intensity distribution $I(q)/c$ for disordered diblock copolymer solutions in the transition region: The dashed and solid lines represent the fits of eq 3 to the experimental profiles for the 4.00 wt % SI4M50/toluene and 1.96 wt % SI4M50/decaline at 20 °C. The superposition of the $I(q)/c$ at low q values was obtained by multiplying the data of the SI4M50/toluene solution by 3.5.

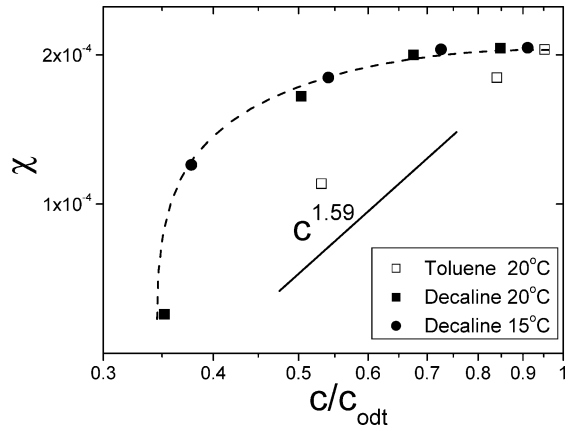

Figure 3. A log−log plot of the effective interaction parameter, χ, vs c/c_{ODT} for the solution of SI4M50 in toluene at 20 °C (□) and decaline at 15 °C (●) and 20 °C (■). The solid line indicates the scaling prediction[7,8] of 1.6, and the dashed line is a guide to the eye.

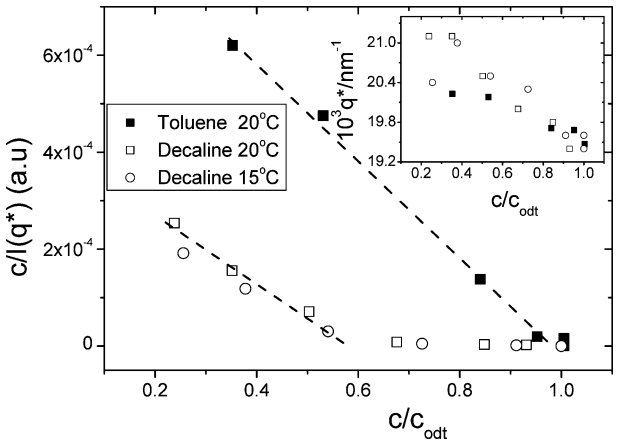

Figure 4. Inverse static structure factor at q^*, $c/I(q)$, vs the normalized concentration, c/c_{ODT}, of SI4M50 in toluene at 20 °C (■) and decaline at 15 °C (○) and 20 °C (□); the dashed line is a guide to the eye. The variation of the characteristic wave vector q^* with reduced concentration of SI4M50 in the two solutions is shown in the inset.

the interactions are simply diluted,[18] and hence the c_{ODT} tends to be shifted toward a higher concentration with increasing temperature, T. Note that χ (for neutral solvent) $= \chi(\text{bulk})\phi_p \sim \phi_p/T$, where ϕ_p is the polymer volume fraction. However, the increase of absolute T brought by the change from 15 to 20 °C is so small that c_{ODT} is hardly affected by this temperature change.

To investigate the origin of the observed differences in the structure factor of SI4M50 sample in these two solvents, the experimental $S(q)$ was represented by

$$S(q) = \frac{N}{F(f,x) - 2\chi N} \tag{3}$$

where N is the number of segments, f the composition, $x = (R_g q)^2$ (R_g is the radius of gyration), and

$$F(f,x) = \frac{N(S_{11} + S_{22} + 2S_{12})}{(S_{11}S_{22} - S_{12}^2)} \tag{4}$$

S_{ij} being the first-order correlation function as given for polydisperse systems.[19] In this fit, the radius of gyration, R_g (=50 nm), the composition $f_{PS} = 0.49$, and the polydispersity parameter assume the same value in both solvents, and only the measure of the segment−segment interactions χ was treated as an adjustable parameter; the former assumption is somehow heuristic considering the different solvent quality but is supported by the similar hydrodynamic radii in dilute solutions. A good fit was accomplished for SI4M50 concentrations in toluene seen in Figure 2 (open points and dashed line) for the 4.00 wt % sample ($<c_{ODT}$). For the same SI in decaline, eq 3 represents well the experimental $S(q)$ in the region $q < q^*$ whereas it leads to systematic deviations at high q values as shown for the 1.96 wt % ($<c_{ODT}$) SI4M50 solution in decaline at 20 °C in Figure 2 (solid points and solid line). This deviation becomes stronger at 15 °C and increases with concentration toward c_{ODT}. In the framework of the blob theory,[7] f should be renormalized according to the solvent selectivity, and in this case, the deviation at $q > q^*$ for the decaline solution is not surprising.

The concentration dependence of the fitted χ parameter is depicted in the double-logarithmic plot of Figure 3. The diblock copolymer solutions in toluene conform to the scaling relation $\chi \sim c^{1.6}$ for diblock copolymer solutions in a common neutral solvent.[7] In contrast, when the solvent of SI4M50 is decaline, χ exhibits a distinctly different c dependence at the examined temperatures, 15 and 20 °C. The unsatisfactory representation of the high-q region of $S(q)$ by eqs 3 and 4 (Figure 2), the different concentration dependence of χ in the solutions of the same SI4M50 diblock (Figure 3), and their different c_{ODT} (Table 1) are nontrivial experimental findings. These effects should be interpreted with respect to the blob theory and the solvent selectivity.[7,8,18]

A fourth effect of the solvent bias relates to the concentration dependence of the peak intensity $I(q^*)$. To account for the different c_{ODT} of the two solutions, Figure 4 shows a plot of $c/I(q^*)$ vs c/c_{ODT} in analogy to the variation of $1/I(q^*)$ with the reduced T_{ODT}/T in block copolymer melts.[9,20−23] The linear dependence of $1/I(q^*)$ with T_{ODT}/T breaks at some $T > T_{ODT}$, signalizing deviations from the mean-field theory. For diblock copolymer solutions in a common solvent, $c/I(q^*)$ vs c displays the anticipated linear dependence up to a certain concentration, $c_x < c_{ODT}$, announcing the onset of the non-mean-field regime for $c > c_x$. However, the value of c_x for the diblock in decaline is much lower ($c_x/c_{ODT} = 0.60$ at 20 °C) than in toluene ($c_x/c_{ODT} = 0.96$)

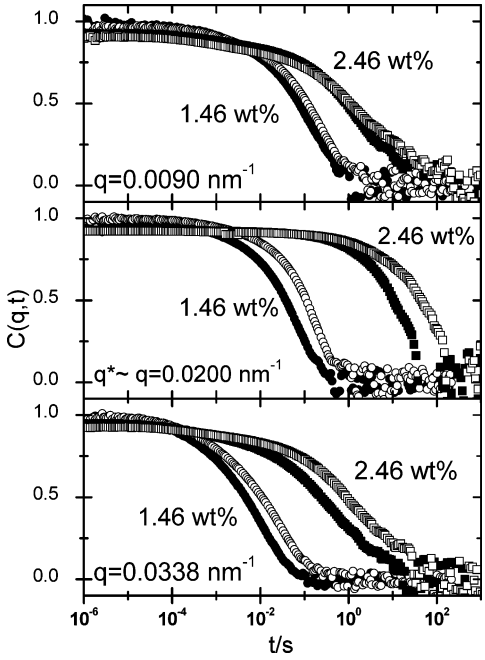

Figure 5. Intermediate scattering functions in two disordered SI4M50 solutions in decaline, 1.46 wt % ($c/c_{ODT} \simeq 0.52$, $q^* = 0.020$ nm^{-1}) and 2.46 wt % ($c/c_{ODT} \simeq 0.88$, $q^* = 0.0195$ nm^{-1}), at the three indicated q's at 15 °C (open) and 20 °C (solid symbols). Circles and squares refer to the 1.46 and 2.46 wt % solutions, respectively.

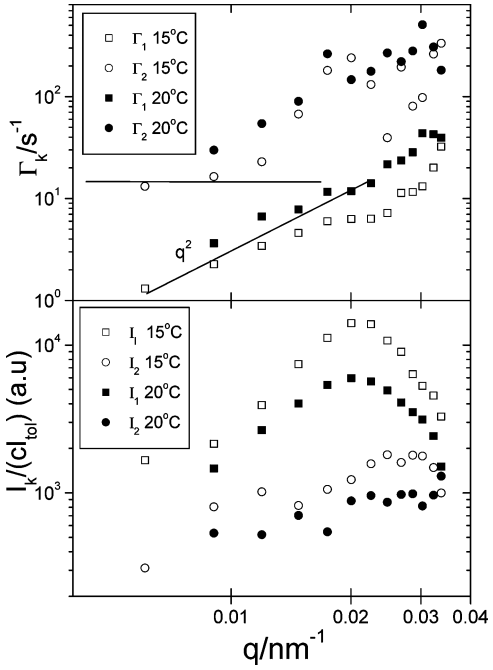

Figure 6. Relaxation rates (upper panel) and intensities (lower panel) for the slow (1) and fast (2) processes in $C(q,t)$ of the 1.46 wt % SI4M50 in decaline. The solid lines are to guide the eye for a diffusive ($\propto q^2$) and q-independent (chain relaxation) rate.

(Table 1). Thus, the increased solvent selectivity for decaline suppresses the c_{ODT} value but enlarges the non-mean-field region with respect to concentration as well. These significant changes induced by the solvent do not reflect substantial variation of the characteristic spacing of the disordered SI4M50 solutions in the two solvents as seen in the inset to Figure 4. q^* exhibits comparable reduction between the two solvents with increasing c toward ODT. The decrease of q^* with c has been reported and addressed in the literature[4] and is attributed to the chain stretching.[20] Based on Figure 4, the value of q^* does not depend on the concentration but on the proximity to ODT expressed by c/c_{ODT}, and at the phase transition, the formed ordered structure has the same characteristic length scale independently of the ODT concentration in the two solvents. We examine next the dynamics of SI4M50 in the two solvents.

B. Dynamic Structure Factor. The intermediate scattering function, $C(q,t)$, that describes the structural relaxation of the diblock copolymer solutions is shown[24] in Figure 5 at three different q values: less than q^*, at q^*, and above q^* ($\simeq$0.02 nm^{-1}) in decaline at 15 and 20 °C. At low q values, the insensitivity of $I(q)/c$ to the temperature variation between 15 and 20 °C (Figures 1 and 2) is nicely reflected in the similar relaxation functions at these temperatures (top part of Figure 5). At $q \geq q^*$, however, $C(q,t)$ changes with temperature, suggesting that the disparity in $S(q \geq q^*)$ between 15 °C and 20 °C is mainly attributed to the dominant slow relaxation mode of $C(q,t)$; note that the measured $G(q,t) = \langle I(q,t)\, I(q)\rangle / \langle I(q)\rangle^2$ is a normalized quantity emphasizing the dominant process. In fact, two main processes were primarily resolved from the distribution $L(\ln \tau)$ (eq 1) with the slow being more sensitive to the temperature variation. The weak contribution at short times due to the cooperative diffusion which is responsible for the relaxation of the total polymer concentration fluctuations[14] is not diblock copolymer specific and hence is not furthermore considered.

The q dependence of the rate, $\Gamma_k(q)$, and intensity, $I_k(q)$, ($k = 1, 2$), of the two processes at 1.46 wt % SI4M50 in decaline are displayed in Figure 6. The characteristic properties of the fast mode (mode 2) are less affected by temperature, and the value of the rate, Γ_2, suggests similar overall chain dynamics as discussed elsewhere.[13,14] It is the slow collective diffusion process (mode 1) that is responsible for the disparity in $S(q \geq q^*)$ at the two temperatures; $C(q,t)$ is more slowed down with decreasing temperature at short ($q > q^*$) than at large ($q < q^*$) length scales. Both the intensity, $I_1(q)$, and the rate, Γ_1, vary with temperature. The proximity to the ODT with decreasing temperature at constant concentration is witnessed by the increase in $I_1(q^*)$ and the slowing down of $\Gamma_1(q^*)$ in Figure 6. For concentrations lower than c_{ODT}, this change cannot be accounted for by the temperature dependence of $\chi_{SI}(T)$ since the SI solutions in toluene at corresponding concentrations are insensitive to such small temperature variations. Instead, it suggests that the increased selectivity of decaline with decreasing temperature lowers the c_{ODT}. An unexpected result is also the effect of temperature on the short ($q > q^*$) length dynamics that probably relate to the enhanced intensity in this high-q region (Figures 1 and 6).

The relaxation function at the higher concentration of 2.46 wt % SI4M50 in decaline, close to the ODT, shows a very similar trend between the two temperatures as for the 1.46 wt % solution (Figure 5). This pretransitional behavior is enhanced with decreasing temperature at constant concentration. At both temperatures, the 2.46 wt % solution is closer to the ODT than the 1.46 wt % solution as indicated by the strong slowing down of the intermediate scattering functions at $q \sim q^*$ shown in Figure 5. Note again that upon decreasing temperature $C(q,t)$ is more slowed down at

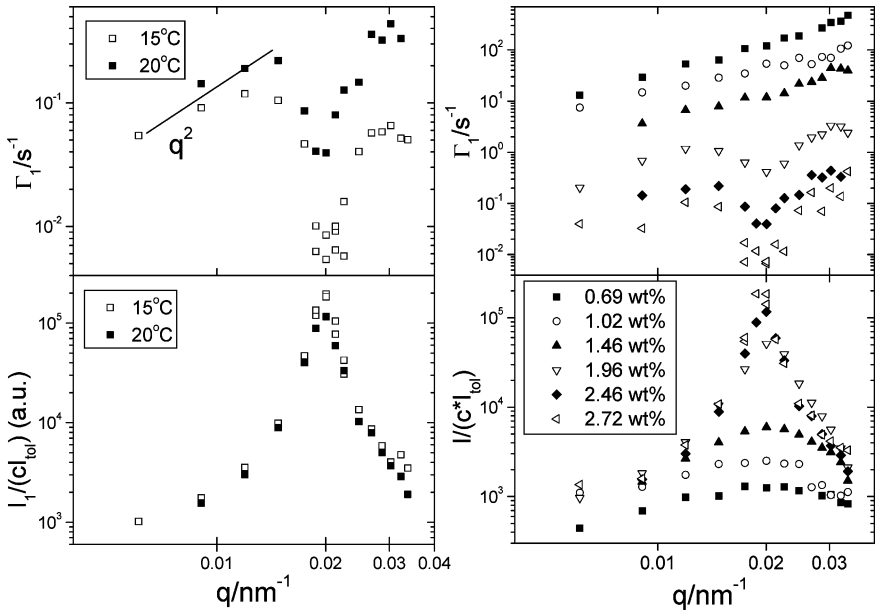

Figure 7. Relaxation rate (upper panel) and intensity (lower panel) for the slow process (1) in 2.46 wt % SI4M50 solution in decaline at 15 °C (open points) and 20 °C (solid points). The evolution of the characteristics of the slow process (1) with concentration is shown in the insets at six different concentrations at 20 °C: 0.69 (■), 1.02(○), 1.46(▲), 1.96(▽), 2.46(◆), and 2.72 wt % (tilted △).

short ($q > q^*$) than at large ($q < q^*$) length scales, and the proximity to the ODT is manifested not only at $q = q^*$ but also at $q > q^*$.

At low q values (0.009 nm^{-1}), the intermediate scattering functions at 15 and 20 °C are very similar, whereas the $C(q,t)$ at 15 and 20 °C are different at the two higher q values of Figure 5. While the disparity at q^* is anticipated by the closer proximity of the system to the ODT at 15 °C, the distinguished difference of $C(q>q^*,t)$ (as for the 1.46 and 2.46 wt % solutions in Figure 5) reflects different microsegregated structures at 20 and 15 °C due to increased selectivity of the decaline solvent. It is noticeable that the difference in Γ_1 at short length scales, i.e., at $q > q^*$, is more pronounced at 2.46 wt % than at 1.46 wt % SI4M50/decaline solution (cf. Figures 5 and 6). The enhanced short wavelength and long-lived fluctuations in these solutions is unexpected and apparently related to the solvent selectivity that probably leads to microdomain structures, solvent lean and solvent rich.

The rate and the intensity of the slow process (mode 1) determined from the distribution relaxation function (eqs 1 and 2) are displayed in Figure 7a for the 2.46 wt % SI4M50 sample in decaline as a function of q at 15 and 20 °C. The characteristics of the fast process (mode 2) are significantly less temperature dependent at this concentration, too (cf. Figure 6). Figures 6 and 7a demonstrate the effect of temperature on the structure and dynamics of diblock copolymer solutions at two concentrations with different proximity to c_{ODT}. For both concentrations, low wavelength composition fluctuations ($q < q^*$) are less affected by the temperature (Figures 5−7), in contrast to the significant effect of the temperature on shorter-range correlations[25] with $q \simeq q^*$. At $q \geq q^*$, the main collective dynamics are clearly retarded by decreasing the temperature by 5 K. Again, this temperature effect is solvent induced. As to the concentration dependence at constant temperature, the characteristic properties ($I_1(q)$, $\Gamma_1(q)$) of the main process (mode 1) exhibit the established behavior[13,14] for moderately polydisperse diblock copolymers displayed in Figure 7b for six different concentrations of SI4M50 in decaline at 20 °C.

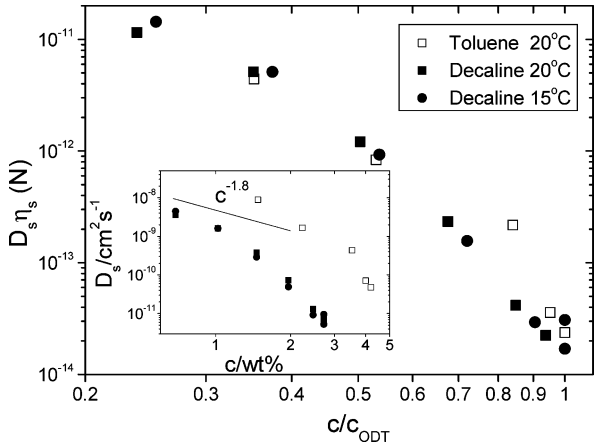

Figure 8. Self-diffusion coefficient D_s in disordered SI4M50 solutions in toluene at 20 °C (□) and decaline at 15 °C (●) and 20 °C (■) vs the reduced concentration c/c_{ODT}. The different solvent viscosity (η_s) was taken into account by plotting $D_s\eta_s$. Inset: the D_s vs SI4M50 concentration for the solutions of the main plot with the theoretical slope (−1.8) for entangled homopolymers in good solvents.

Returning to the low q-dynamics, $C(q,t)$ yields the chain self-diffusion[26,27] $D_s = \Gamma_1/q^2$ since at $q < q^*$, $S(q)$ arises from composition polydispersity responsible for the incoherent scattering. We have recently found that D_s senses the proximity to ODT undergoing an excess fluctuation-induced thermodynamic slowing down.[13] Figure 8 visualizes the relation of $D_s\eta_s$ (corrected by the different solvent viscosity η_s) to the reduced concentration c/c_{ODT} in the SI4M50/toluene and SI4M50/decaline solutions. For comparison, a D_s vs c plot is shown in the inset to Figure 8. The same SI4M50 chain diffuses slower (taking into account their η_s's) in decaline than in toluene at the same polymer concentration. Deviation from the good solvent scaling low ($c^{-1.8}$) in the case of the decaline solution cannot be attributed to the solvent quality; a steeper dependence would be expected[27] for

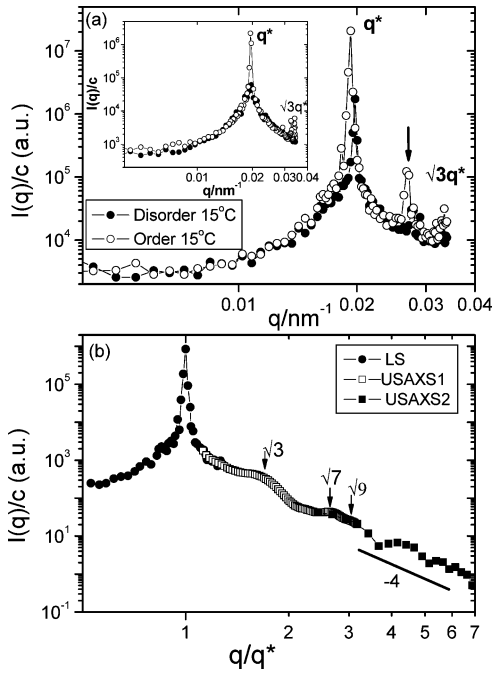

Figure 9. (a) Intensity distribution $I(q)/c$ for disordered (●) and ordered (○) SI4M50 2.72 wt % solution in decaline at 15 °C obtained from light scattering (LS). The higher order peak at $\sqrt{3}q^*$ appears at the edge of the LS q's, and the peak indicated by the arrow is explained in the text. Inset: $I(q)/c$ for disordered (●) and ordered (○) SI4M50 4.22 wt % solution in toluene at 20 °C. (b) $I(q)/c$ profiles for the ordered SI4M502.72 wt % solution in decline at 15 C from USAXS measurements are superimposed to the LS $I(q)/c$ profile of (a) and shown as a function of the normalized q/q^* over an extended q range.

D_s in Θ solvents. The resulted superposition in the main plot of Figure 8 is remarkable if we consider the different solvent quality, c_{ODT} values, and hence the extent of the topological constraints (entanglements) in the two solutions; the overlap concentration $c^* \sim 0.3\%$.

The retardation of the low-q dynamics is weaker compared to the slowing down of the structural relaxation (Γ_1) at q^* approaching ODT either by increasing concentration (Figures 6 and 7) or by decreasing temperature (Figure 7); at q^* the structure factor assumes its maximum $S(q^*)$. For the former dynamics, the empirical expression $D_s \sim \exp(-\alpha\chi N)$ (with $\alpha \simeq 0.1$) was proposed,[13,28] whereas for the latter $\Gamma_1(q^*) \sim (\chi_s - \chi)N$ with $2\chi_s N = F(f,\chi)$ of eq 4. In fact, the dynamics associated with the order parameter fluctuations at q^* is a sensitive index of the microphase separation, and hence the assignment of mode(1) to the structural relaxation is justified.

C. Two-Phase Coexistence. Two coexisting phases can be found in the SI4M50 solutions both in decalin at 2.72 wt % at 15 °C and in toluene at 4.22 wt % at 20 °C. The two phases, ordered and disordered, are as close to the phase transition as possible for the two regimes. The two-phase regions, in both solvents, are only found in a very small concentration range (∼0.1 wt %) similarly to the case of bulk block copolymers for which the two-phase coexistence was observed[9] over a very narrow temperature range. The nature of the two-phase region gives us the possibility to investigate any immediate change in the dynamic response crossing the phase boundary without any substantial change in concentration.

In Figure 9, the static structure factors are displayed for the two phases in decaline (a) for the 2.72 wt % SI4M50 sample at 15 °C and in toluene (inset to Figure 9a) for the 4.22 wt % SI4M50 sample at 20 °C. It should be noted that the peak in the disordered phase at 15 °C in decaline is narrower than the peak (not shown) for the same solution at 20 °C. In the ordered phase, in both solvents, a second-order peak can just be revealed (Figure 9a) at the high-q edge of the light scattering q range. It is a high order maximum at $q/q^* = \sqrt{3}$, suggesting a hexagonal microdomain structure, compatible with the displayed birefringence of the ordered solution. The peak at $q \approx 0.028$ nm^{-1} (arrow in Figure 9a) in the ordered samples, clearly seen in decaline, is an artifact due to the reflection of the diffracted light (from the ordered structure) to the cylindrical cell wall and appears for well-ordered phases. The peak intensity $I(q^*)$ is anisotropic in the sense that maximum is attained by proper orientation of the grains relative to the direction of the momentum transfer vector q.

Microphase-separated symmetric diblock copolymers in the undiluted state form a lamellar morphology. To verify the present deviation, the intensity profile $I(q)$ of the same SI4M50 diblock in decaline at 2.7 wt % and 15 °C was extended at high q's by performing USAXS measurements. Two USAXS profiles were superposed to the light scattering $I(q)$ profile (Figure 9a) by a vertical shift in the log $I(q)$ vs log(q/q^*) plot of Figure 9b. Over the extended q range $I(q)$ exhibits multiple order scattering maximum at $q/q^* = 1$, $\sqrt{3}$, $\sqrt{7}$, and $\sqrt{9}$ characteristic of hexagonal cylinders (hex-cyl). Further, the observed q^{-4} power (Porod's) low implies a sharp interface for the hex-cyl.

From the position of the first-order peak, q^*, the Bragg spacing, d, of the hexagonal structure can be calculated; $d = 2\pi/q^*$. It is also clear from the q^{-4} dependence in the USAXS spectrum (Figure 9b) that there is a sharp interface between the polystyrene and polyisoprene microphases in the hexagonal cylinders. If we assume a complete segregation of PS and PI block into PS and PI domains, respectively, the total volume fraction of the polystyrene phase, $\phi_{PS} = f_{PS}\phi_p + y\phi_{sol}$; f_{PS} is the volume fraction of neat diblock copolymer (Table 1), ϕ_p the total volume fraction of the polymer, ϕ_{sol} the total volume fraction of the solvent, and y the fraction of the solvent resided in the PS microphase. Using this expression for the volume fraction of the PS phase, the value of d and geometrical packing for the inner radius, R, of the cylinders is given by

$$R = \sqrt{\frac{2\phi_{PS}}{\pi\sqrt{3}}}\, d \tag{5}$$

The interfacial area in a hexagonal phase is thus the area of the inner cylinder (PS phase) with the radius R. If only the block copolymer participates in the interface (sharp interface), the area per block copolymer, a_p, reads

$$a_p = \sqrt{2\phi_{PS}\pi\sqrt{3}}\,\frac{v_p}{d\phi_p} \tag{6}$$

where v_p is the molecular volume for the neat block copolymer.

For the SI4M50 in toluene and decaline at ODT, the Bragg spacing is $d = 324$ nm. For the estimation of a_p the solvent distribution in toluene has to be addressed. For a literally neutral solvent for both PS and PI, y can be set equal to 0.5; a slight deviation from the neutrality

would affect the solvent partition, but in any case, $0.4 < y < 0.6$. Using eq 6, $\phi_p = 0.037$, $y = 0.49$, and $\nu_p = 6070$ cm^3, the area per chain molecule for the toluene system was calculated to be $a_p = 584$ nm^2. It has been shown[29,30] that for a given morphology the area per molecule for a specific block copolymer does not change significantly (±15%) with solvent and concentration. For the SI4M50/decaline system it is found that about 25% of the decaline is allocated in the PS phase; $y = 0.025$ ($\phi_p = 0.0265$) and 0.22 ($\phi_p = 0.0247$) at 20 and 15 °C, respectively. The increase of the solvent segregation was expected since the solvency for PS decreases with decreasing temperature. The lower c_{ODT} in decaline than in toluene (Table 1) is also attributed to the solvent selectivity. However, no micelles were observed approaching ODT.

Aside the sharp peak at q^*, the intensity profile in the ordered phase displays an additional broad peak centered at q^*. Different origins are conceivable. Diffusive scattering may arise from the coupling of the order parameter (composition) to the layer displacement $u(r)$. For oriented samples[31,32] with 1D lamellar morphology along z

$$I(q_z) \propto \sum_n \int dr_\perp \exp(iq_z nd)\langle \exp[-iq_z(u_n(r_\perp) - u_0(0))]\rangle \quad (7)$$

where q_z is along the layer normal, and the significant displacements $u_n(r)$ for the nth layer are along q_z. A sharp peak with strong $I(q^*)$ is observed when the periodic structure is perpendicular to q in the ordered phase, and the second exponential term is responsible for the broadening of the diffraction peak. In the present case, however, the profile of the broad peak of $I(q)$ is insensitive to the orientation of the sample and hence very similar to the diffuse scattering from the disordered phase. On the basis of this observation, one-dimensional layer displacements along z-direction cannot account for the broad diffuse scattering around q^*.

A second possibility is that the broad component of the diffraction maximum at q^* in the ordered region arises either from (i) thermal fluctuations causing undulations of the sharp interfaces in the ordered state[33] or (ii) coexistence of the ordered and disordered phases[9] in the volume irradiated by the laser. The former should be absent in the disordered region in contrast to the experimental evidence (Figure 9a). We could also rule out the latter (ii) origin only on the basis of the SI4M50 in toluene shown in the inset to Figure 9a. However, one can discern a sharp component on the top of the broad component in the static scattering profile from the disordered region in the main Figure 9a. Access to the dynamic structure factor $S(q,t)$ in the two phases helps elucidate the nature of these fluctuations.

From the correlation functions,[24] $C(q,t)$, in Figure 10a (decaline) and Figure 10b (toluene) the similarity between the $C(q,t)$ of the different phases is noticeable at low q values for two phases in decaline at 2.72 wt % and toluene at 4.22 wt % SI4M50. This indicates that the large-scale relaxation behavior does not change between the ordered and disordered state close to the ODT even though the coherence length (inverse of the half-width at half-maximum of $I(q^*)$) changes due to microphase separation. In the ordered phase, for both the decaline and toluene samples, a clear slowing down of $C(q,t)$ at $q > q^*$ compared to the disordered phase is

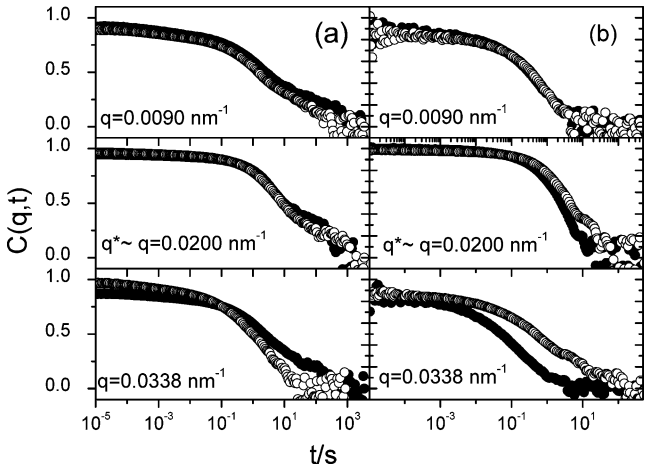

Figure 10. Intermediate scattering functions, $C(q,t)$, in disordered (○) and ordered (●) SI4M50 solutions in (a) decaline 2.72 wt % at 15 °C and (b) toluene 4.22 wt % at 20 °C, at three different q's.

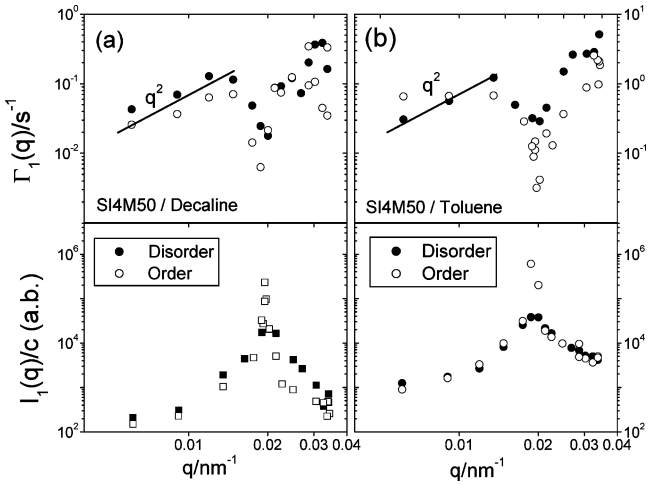

Figure 11. Relaxation rates (upper panel) and intensities (lower panel) for the slow (1) process in $C(q,t)$ of disordered (●) and ordered (○) SI4M50 solutions in (a) decaline 2.72 wt % at 15 °C and (b) toluene 4.22 wt % at 20 °C.

visible. This apparent slowing down of the rates is an effect of the second-order peak increasing the contribution of the slow process (mode 1) to $C(q,t)$.

The evaluated rates and intensities from ILT for the two coexistent phases are shown in Figure 11a (decaline) and Figure 11b (toluene) as a function of q. A similar behavior between the two phases can be seen at low q's both for the rates and intensities. This indicates a similar long-range dynamic behavior in both the ordered and disordered state. The thermodynamic slowing down of the rates at q^* are slightly enhanced in the ordered phase for both solvents. The corresponding intensities have increased far more relative to the slowing down of the rates.

IV. Concluding Remarks

The present experimental study of the static and dynamic structure factor in both disordered and ordered regions in the solutions displaying the order−disorder coexistence in an ultrahigh molecular weight symmetric diblock copolymer yields new information for the ordering region and the effect of solvency.

(i) Based on the position of the multiple order scattering in the static structure factor $S(q)$ (Figure 9),

hexagonally arranged cylinders and not lamellar layered structure is the adopted morphology of the ordered regions in the solutions in contrast to the undiluted state. Violation of the solvent neutrality leads to an effective asymmetric block copolymer composition as a consequence of renormalization of the solvent selectivity.

(ii) At the order−disorder transition ODT, reached by either increasing concentration at constant temperature or decreasing temperature at constant concentration, a coexistence of two phases is clearly observed in the two examined solvents. Based on the form of $S(q)$ and the dynamic structure factor $S(q,t)$ (Figures 9 and 10), there are significantly dynamic fluctuations on both sides of the peak position of $S(q)$ at q^*. The ordered phase is distinguished both by the sharp $S(q^*)$ peak and the associated slow dynamics. The latter exhibit the well-established thermodynamic slowing down effect[4,11−13] at q^*. The chain diffusivity D_s obtained from the $S(q,t)$ at low q ($<q^*$) undergoes the recently reported[13] thermodynamic slowing down with increasing concentration in the non-mean-field regime.

(iii) In the disordered region near ODT, slight solvent selectivity enlarges the non-mean-field region (Figure 4), enhances the short ($q > q^*$) length fluctuations (Figures 1 and 2), and leads to deviation from the scaling relation of the interaction parameter χ with concentration (Figure 3) under neutral solvent conditions. The effective χ depends on the solvent selectivity.

Acknowledgment. The financial support of the EU (Grant FMRX-CT97-0112) is gratefully acknowledged.

References and Notes

(1) Lodge, T. P.; Pudil, B.; Hanley, K. J. *Macromolecules* **2002**, *35*, 4707.
(2) Hanley, K. J.; Lodge, T. P.; Huang, C.-I. *Macromolecules* **2000**, *33*, 5918.
(3) Wanka, G.; Hoffmann, H.; Ulbricht, W. *Macromolecules* **1994**, *27*, 4145.
(4) Chrissopoulou, K.; Pryamitsyn, V. A.; Anastasiadis, S. H.; Fytas, G.; Semenov, A. N.; Xenidou, M.; Hadjichristidis, N. *Macromolecules* **2001**, *34*, 2156.
(5) Jönsson, B.; Lindman, B.; Holmberg, K.; Kronberg, B. *Surfactants and Polymers in Aqueous Solution*; John Wiley & Sons: London, 1998.
(6) Laughlin, R. G. *The Aqueous Phase Behavior of Surfactants*; Academic Press: London, 1994.
(7) Fredrickson, G. H.; Leibler, L. *Macromolecules* **1989**, *22*, 1238.
(8) Whitmore, M. D.; Noolandi, J. *J. Chem. Phys.* **1990**, *93*, 2946.
(9) Koga, T.; Koga, T.; Hashimoto, T. *J. Chem. Phys.* **1999**, *110*, 11076.
(10) Hadjichristidis, N.; Iatrou, H.; Pispas, S.; Pitsikalis, M. *J. Polym. Sci., Part A: Polym. Chem.* **2000**, *38*, 3211.
(11) Semenov, A. N.; Anastasiadis, S. H.; Boudenne, N.; Fytas, G.; Xenidou, M.; Hadjichristidis, N. *Macromolecules* **1997**, *30*, 6280.
(12) Sigel, R.; Pispas, S.; Hadjichristidis, N.; Vlassopoulos, D.; Fytas, G. *Macromolecules* **1999**, *32*, 8447.
(13) Holmqvist, P.; Pispas, S.; Hadijichristidis, N.; Fytas, G.; Sigel, R. *Macromolecules* **2003**, *36*, 830.
(14) Holmqvist, P.; Pispas, S.; Hadjichristidis, N.; Fytas, G.; Sigel, R. *Macromolecules* **2002**, *35*, 3157.
(15) Koga, T.; Hart, M.; Hashimoto, T. *J. Appl. Crystallogr.* **1996**, *29*, 318.
(16) This factor can be rationalized by the larger contribution of the light scattering from total polymer concentration fluctuations (cooperative diffusion) in decaline due to higher optical contrast and lower solvent quality as compared to those of toluene.
(17) Sigel, R.; Pispas, S.; Vlassopoulos, D.; Hadjichristidis, N.; Fytas, G. *Phys. Rev. Lett.* **1999**, *83*, 4666.
(18) Hashimoto, T.; Mori, K. *Macromolecules* **1990**, *23*, 5347.
(19) Burger, C.; Ruland, W.; Semenov, A. N. *Macromolecules* **1990**, *23*, 3339.
(20) Rosedale, J. H.; Bates, F. S.; Almdal, K.; Mortensen, K.; Wignall, G. D. *Macromolecules* **1995**, *28*, 1429.
(21) Hashimoto, T.; Shibayama, M.; Kawai, H. *Macromolecules* **1983**, *16*, 1093.
(22) Hashimoto, T.; Tsukahara, M.; Kawai, H. *Polym. J.* **1983**, *15*, 699.
(23) Sakamoto, N.; Hashimoto, T. *Macromolecules* **1995**, *28*, 6825.
(24) The low statistics near the baseline of the scattering functions is partial due to the low laser intensity (∼5 mW) in order to avoid patterns formation during data accumulation (Sigel, R.; et al. *Science* **2002**, *297*, 67).
(25) The strong slowing down of Γ_1 at $q \sim q^*$, apart from the larger involved error due to the very slow dynamics, is not fully ascribed to the increase of $S(q^*)$ (cf. Figure 7a for the two displayed temperature). Phenomenologically, this is attributed to the nonlocal kinetic Onsager coefficient as has been reported for hard (Segre, P. N.; Pusey, P. N. *Phys. Rev. Lett.* **1996**, *71*, 776) and soft sphere (ref 17) colloids.
(26) Jian, T.; Anastasiadis, S. H.; Semenov, A. N.; Fytas, G.; Adachi, K.; Kotaka, T. *Macromolecules* **1994**, *27*, 4762.
(27) Anastasiadis, S. H.; Chrissopoulou, K.; Fytas, G.; Appel, M.; Fleischer, G.; Adachi, K.; Gallot, Y. *Acta Polym.* **1996**, *47*, 250.
(28) Lodge, T. P.; Dalvi, M. C. *Phys. Rev. Lett.* **1995**, *75*, 657.
(29) Olsson, U.; Wennerström, H. *Adv. Colloid Interface Sci.* **1994**, *49*, 113.
(30) Alexandridis, P.; Olsson, U.; Lindman, B. *Langmuir* **1997**, *13*, 23.
(31) Gunther, L.; Imry, Y.; Lajzerowicz, J. *Phys. Rev. A* **1980**, *22*, 1733.
(32) Holyst, R. *Phys. Rev. A* **1990**, *42*, 7511.
(33) Stepanek, P.; Nellet, F.; Almdal, K. *Macromolecules* **2001**, *34*, 1090.

MA049702P